Proceedings of the 21st ICSMGE, Vienna, Austria, 14 – 19 June 2026. Pistrol, Adam & Schweiger (eds.)
Published by: ÖGG, Austrian Society for Geomechanics, Salzburg, Austria, ISBN 978-3-9503898-4-5
https://doi.org/10.53243/ICSMGE2026-203

Modeling of internal erosion with equations for a two-phase flow in analogy to flow of air and water using the Mixed Finite Element Method

Luisa Kagermeier, Eugen Perau, Abdulsalam Abdulrahman, Jonas Hülsbusch
Institute of Geotechnical Engineering, University Duisburg-Essen, Essen, Germany, luisa.kagermeier@uni-due.de

Two-phase flows in granular soils are important in many geotechnical fields. In one case the two phases may be air and water, in another case they may be eroded particles and water. Examples of geotechnical applications of air and water flow include flow in dikes and compressed air tunnelling. An example of the movement of particles and water is the process of internal erosion of soils. This is of particular interest in relation to the stability and the durability of dikes and dams. The description of such processes requires differential equations in order to formulate specific initial boundary value problems. This paper sets out a new approach to describe internal erosion as a process. However, it is important to note, that most of the older approaches can only be used to describe depict states. In order to describe the movement of soil particles, a mechanical approach must be employed. This approach, working with the two phases water and eroded particles can be implemented analogous to the two-phase flow of water and air. To achieve this objective, an approach is hereby presented that is based on the Theory of Porous Media. To solve the system of differential equations, a separate software system based on the Mixed Finite Element Method with Raviart-Thomas elements is presented, which can be used to solve initial boundary value problems of two-phase flows with water and air. The existing modular program code has been extended to include a preprocessor in MS-Excel, which can be used to formulate initial and boundary value problems without programming knowledge. The results of some selected examples of two-phase flows are presented. Based on this, the analogies and differences between the two-phase flow of particles and water are demonstrated. The focus is on the additional term required to describe dispersion in particle flow.

KEYWORDS: internal erosion, suffusion, water, particles, air, two-phase flow, dispersion, Mixed Finite Element Method

1 INTRODUCTION

The simultaneous flow of two phases in soil is important in various areas of geotechnical engineering. The two phases can be air and water, but also dissolved soil particles and water. One example of a geotechnical application is the flow through dykes and dams (Sharp et. al., 2013). In order to evaluate the stability of leaking dams and dykes, it must be investigated whether they are susceptible to internal erosion (BAW 2013a/b).

The term ‘internal erosion’ is often used as a generic term for all erosive processes that take place within the soil. This includes suffusion (van Beek, 2015), which describes the process of rearrangement and transportation of soil particles within the grain skeleton of a soil. As shown in Figure 1a, only the fine components of a soil are dissolved and transported through the pore channels of the grain skeleton.

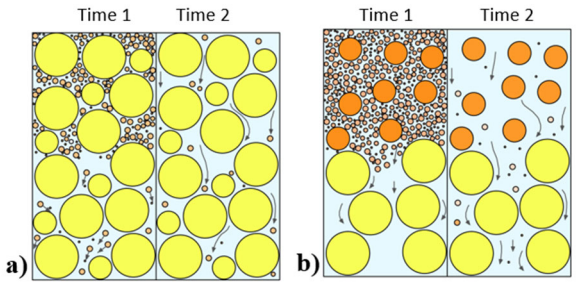

Figure 1. Internal erosion processes, presented in two time steps:
a) inner suffusion due to downward flow of water,
b) contact suffusion (according to Ziems (1968))

An unconditional requirement for internal erosion is that the particles are small enough to pass through the pore constrictions and that there is a corresponding groundwater flow (Wan & Fell, 2008). If the process of suffusion, as shown in Figure 1b, takes place at the boundary between two soils layers, where one of it consists of rather coarse grains and the other of rather fine grains, it is referred to as ‘contact suffusion’. Due to groundwater flow fine soil particles can migrate from the fine soil into the adjacent coarse-grained soil. This is known as ‘colmation’.

Ziems (1968) categorized contact suffusion into different types based on experimental investigations. These types, shown in Figure 2, differ in the arrangement of the two soil layers in relation to the direction of gravity and the flow direction of the water. The arrows in Figure 2 represent the direction of flow of water.

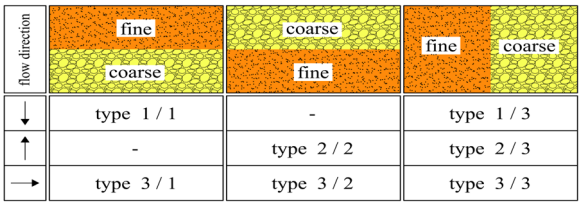

Figure 2. Types of contact suffusion according to Ziems (1968)

Defining the types in this way, however, only strictly vertical and horizontal layer sequences and flow directions are taken into account. This means an enormous simplification for real geotechnical problems with other orientation of layers and groundwater flow. In addition, this typification only allows initial states to be represented in the sense of design rules but no representation of ongoing processes.

In order to describe the movement of soil particles in the subsurface as a process, it is necessary to use approaches based on mechanics. In a simple variant, Askamp (2024) describes internal erosion as a two-phase flow in a rigid grain skeleton, restricting it to suffusion and colmation. In this case, the two flowing phases are the groundwater and the fine particles.

The two-phase flow (water/particles) can be described in principle analogous to other two-phase flows, especially that of air and water in soils, as for example in Perau (2001). In this case, the formulation used in Potthoff (2003) with the Mixed Finite Element Method and an associated program code can also be used for the numerical solution of the associated initial boundary value problems.

However, it must first be proven that the mechanical model (Perau, 2001) and its numerical implementation (Potthoff, 2003) for the flow of air and water lead to plausible solutions in the simulation of initial boundary value problems. This is done through the exemplary calculation and discussion of examples.

2 TWO-PHASE FLOW OF AIR AND WATER

To describe the two-phase flow of air and water in soil, Perau (2001) used the well-established Theory of Porous Media (cf. e.g. Ehlers, 1989). The associated system of differential equations essentially contains the conservation equations for masses and momentum of the individual phases. Some of the variables have to be determined by constitutive equations.

2.1 *Mechanical model*

As in Perau (2001), the model is specified to describe a two-phase flow in a rigid grain skeleton (S). Then, only the conservation equations of the two phases water (F) and air (G) are evaluated to describe the movement of the two fluids. The two phases are regarded as immiscible fluids, with water being assumed as incompressible and air as compressible according to the law of Boyle-Mariotte. The spatial and temporal distribution of the phases, the 'constituents' (k), is represented by their respective volume fractions (n_k). The sum of all three volume fractions must be equal to one according to the following equation, the so-called 'saturation equation':

$$n_F + n_S + n_G = 1 \tag{1}$$

The equation for the conservation of mass reads for phase k with k ϵ {F,G} as follows:

$$\rho_{kR} \cdot n_k + div\left(\mathbf{w_k}\right) - m_k = 0 \tag{2}$$

where ρ_{kR} is the real density, $\mathbf{w_k}$ the vector of mass flow density [kg/m²s] and m_k the mass exchange of the respective constituent k. Since mass exchange between the two phases water and air is excluded, $m_k = 0$ has to be applied.

Neglecting inertia forces, the following vectorial equation describes the conservation of momentum:

$$div\mathbf{T}_k + n_k \cdot \rho_{kR} \cdot \mathbf{b} + \mathbf{s_k} - \dot{\mathbf{x}}_\mathbf{k} m_k = 0 \tag{3}$$

where $\mathbf{T}_k$ is the stress tensor, **b** the external acceleration to cover gravity body forces and $\mathbf{s}_k$ is the exchange of momentum which describes effects like seepage forces. In Eq. 3 also the velocity of the respective constituent $\dot{\mathbf{x}}_\mathbf{k}$ is involved, which can be transferred to the mass flow density $\mathbf{w}_k$ as follows in Eq. 4:

$$\mathbf{w}_k = \rho_{kR} \cdot n_k \cdot \dot{\mathbf{x}}_\mathbf{k} \tag{4}$$

With Eq. 4 the velocity in Eq. 3 can be replaced to receive:

$$div\mathbf{T}_k + n_k \cdot \rho_{kR} \cdot \mathbf{b} + \mathbf{s_k} - \frac{m_k}{\rho_{kR} \cdot n_k} \mathbf{w}_k = 0 \tag{5}$$

The equations of motion have to be supplemented by constitutive equations describing the mechanical behavior of the individual constituents and their mechanical interaction. In this way, the stress tensor ($\mathbf{T_k}$) and the interaction term ($\mathbf{s_k}$) have to be defined. The following applies to the interaction term:

$$\mathbf{s}_k = \mathbf{s}_{k0} + \mathbf{s}_{kE} \tag{6}$$

where $\mathbf{s_{k0}}$ is defined analogue to Ehlers (1989) or Perau (2001) and is not in focus here and $\mathbf{s_{kE}}$ is defined as follows in Eq. 7. In Eq. 7 is set up, that the interaction forces between the constituents are proportional to the relative velocities of the constituents. The factors of the proportion R_{ij} were called resistivities (Perau, 2001) and could be understood as a generalization of a reciprocal value of the permeability as first recognized by Raats (1969).

$$\mathbf{s}_{kE} = -R_{kj} \cdot \left(\dot{\mathbf{x}}_\mathbf{k} - \dot{\mathbf{x}}_\mathbf{j}\right) - R_{ki} \cdot \left(\dot{\mathbf{x}}_\mathbf{k} - \dot{\mathbf{x}}_\mathbf{i}\right) \tag{7}$$

From Eq. 7 with Eq. 4 we get:

$$\mathbf{s}_{kE} = -R_{kj} \cdot \left(\frac{\mathbf{w}_k}{\rho_{kR} \cdot n_k} - \frac{\mathbf{w}_j}{\rho_{jR} \cdot n_j}\right) - R_{ki} \cdot \left(\frac{\mathbf{w}_k}{\rho_{kR} \cdot n_k} - \frac{\mathbf{w}_i}{\rho_{iR} \cdot n_i}\right) \tag{8}$$

Including the resistivity terms for R_{kj} and R_{ki}, which have to be specified later in detail, these terms $\mathbf{s}_{kE}$ describe the exchange of momentum between the three phases involved by their penetration process. For two-phase flow of water and air these terms are presented in Perau (2001).

2.2 *Numerical implementation*

In order to solve boundary value problems for two-phase flow of water and air due to the approaches of Perau (2001) a numerical solution had been derived, which is still in use. Potthoff (2003) applied the Mixed Finite Element Method. In contrast to the conventional FEM, here shape functions are formulated not only for the scalar process variables, but also for the vector-valued flows (see e.g. Starke, 2000).

As described with more details in Potthoff (2003) and Korsawe et al. (2003) the lowest-order approach of Raviart-Thomas elements (RT_0) has been used relying on two scalar process variables as well as the two mass flow densities as vectorial process variables.

The state of the system during the time is determined by the two scalar variables of the real density of the air (ρ_{GR}) and the volume fraction of the water (n_F) and the two mass flow densities of air ($\mathbf{w_G}$) and water ($\mathbf{w_F}$).

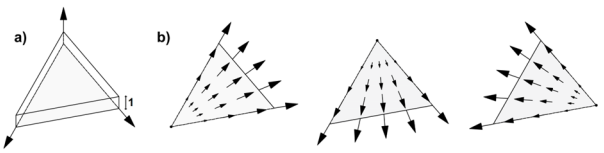

Figure 3. Shape functions after Raviart & Thomas (1977) for a triangular element RT_0: a) for the scalar variables, b) for the vector-valued variables

Figure 3 shows the shape functions for the two scalar process variables ρ_{GR} and n_F, set to be constant on each element, as well as the shape functions for the vectorial process variables of the used RT_0-elements, used for $\mathbf{w_G}$ and $\mathbf{w_F}$. Here the normal component of the vector at the edge of an element is either zero or one. For more details for this 2D-solution as for a simple 1D-solution see Potthoff (2003).

While Potthoff's program in MATLAB concentrates on the assembling of matrices and the solution of the respective non-linear system of equations, Perau & Kagermeier (2024) presented a preprocessor, created in MS-Excel. In this type of MS-Excel files data are given to define the initial boundary value problem and to control the calculation. It contains tables to define the geometry and assignment of material groups, a soil database and a function data base in order to define initial and boundary conditions. This enables the user also to run the program even with parameterized initial boundary value problems to vary geometry or material parameters. Also, the discretization in time and space can be governed by input data. Finally, also some output features can be controlled.

The main steps of the procedure are listed in Perau & Kagermeier (2024) as well as the documentation of some simple initial boundary value problems with water and air flow in a 1D-cylinder. These examples have proofed the basic applicability of the approaches, the numerical implementation and the pre-processor. In the meantime, some 2D-problems have been considered, whose results are presented and discussed as follows here.

3 CALCULATION EXAMPLES ON A DIKE

To show the usefulness of the equations from Perau (2001) and the program code of Potthoff (2003), some examples which are relevant to practice are presented. For all examples here, a soil material is used which is called 'sand' by Potthoff (2003, p. 94) and whose geo-hydraulic properties could be more exactly described as 'slightly silty fine sand'.

The program investigates the movement of both flowing fluids – water and air. Here, the presentation of the results concentrates on the volume fraction of the water n_F and the flow of water $\mathbf{w}_F$, since for dikes these are the relevant variables. For further examples, where flow and densities of air are more relevant it is referred to Perau & Kagermeier (2024).

Since for a two-phase flow of air and water the local degree of saturation S plays an important role, the most related variable, the volume fraction of water n_F is in focus of the presented results. n_F is defined as $S \cdot n$, where n is the void ratio, which is the volume fraction of the pores.

Figure 4. Color scale for the volume fraction n_F

Figure 4 presents for all examples the color scale for the volume fraction of water n_F, which ranges from blue for $n_F = 0$ to red for $n_F = 0.36$, which is the volume fraction of the pores. Hence, blue stands for dry and red for fully water saturated soil.

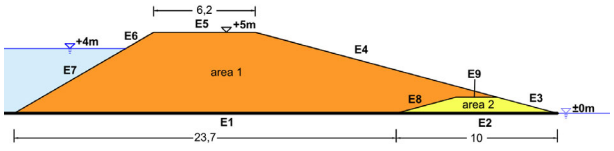

Figure 5. Example 1 - Cross-section of the dike with water levels

Figure 5 shows the structure and dimensions of Example 1, where flow through a dike is simulated. Generally, the dike consists of two areas: the supporting body (area 1, orange) and the foot filter (area 2, yellow). The material of the supporting body remains as 'sand' for all calculations. The material of the foot filter is modified in changing the permeability (k) of the material. For sake of simplicity, all other soil parameters remain unchanged.

For all examples, the initial condition (t = 0) for the entire dike body is set as follows: density of air ρ_{GR} is associated to atmospheric air pressure, volume fraction of water $n_{F,t=0} = 0{,}05 \cdot n$ associated to water saturation of 5%, mass flow densities for both fluids are initially zero ($\mathbf{w}_{G,t=0} = \mathbf{w}_{F,t=0} = \mathbf{0}$).

The boundary condition on the left side of the dike (E7) is a sudden rising of the water level from 0 m to a height of 4 m at t = 0 like presented in Figure 5. The dike is placed on an impermeable layer (edges E1 & E2), which is represented by a natural boundary condition. According to the initial conditions, atmospheric air pressure and $n_{F,t=0} = 0{,}05 \cdot n$ are applied as boundary conditions to the boundaries which are exposed to air (edges E3 to E6). For the left slope (edge E7), atmospheric pressure is applied as a boundary condition at the groundwater level, which increases hydrostatically with depth. Here, the volume fraction of water is $n_F = n$.

The FEM simulation was carried out with triangular Raviart-Thomas elements RT_0 with different element sizes. Note, that with RT_0-elements the volume fraction of water, n_F as a scalar variable is represented only by one single value on each element, according to Fig. 3a, that means one color per element. For illustrations in this article a coarser mesh was employed in order to facilitate the representation of the distribution of the volume fraction of Water, n_F and the water flow density as one arrow per element.

3.1 *Example 1A – Homogeneous Dike during the time*

In the first Example 1A a homogeneous dike is under consideration. That means, the 'sand' is used as material for both areas shown in Figure 5.

Figure 6 presents the results of this simulation at various points in time. It can be seen that the expected infiltration of the dike body occurs after a certain time (Figure 6b). The infiltration front advances across the width of the dike, whereby water also leaks out on the air side. The saturated zone (red color), which is implemented in the lower and left area of the dike is confined by a moving free surface with a capillary zone. With the full penetration of the dike water flows out of the dike at the air side. After around 40 hours a stationary state is reached.

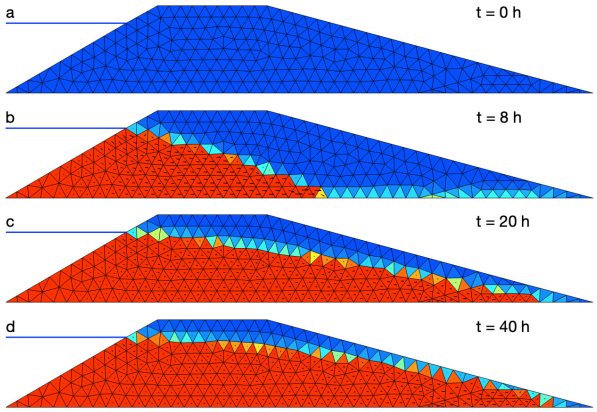

Figure 6. Example 1A - homogeneous dike - volume fraction of water (n_F) at different times with colors according to Figure 4

3.2 *Variation of the foot filter permeability*

In order to investigate the effect of the permeability of area 2, where in practical cases the filter material should appear, two further calculations were run. In **Example 1B**, the permeability of area 2 has been reduced by a factor of 100. This could be, for example, the result of a process in which the foot filter is clogged by a massive inflow of small particles, called 'colmation'.

In **Example 1C**, the permeability was increased by a factor of 100 compared to the sand material, in order to simulate the effect of a foot filter like it is recommended for dike constructions. Figure 7 shows a detail of the geometry and for the three Examples 1A, 1B and 1C the section of the foot filter at time step t = 40 h where a stationary flow has been reached.

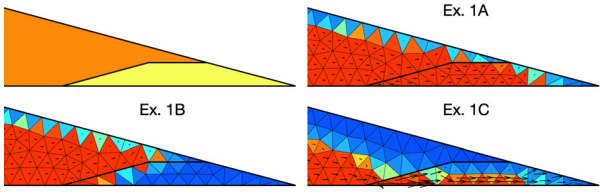

Figure 7. Variation in the filter permeability – the colors represent the volume fraction of water (n_F), the arrows represent the mass flow density of water ($\mathbf{w}_F$) for time t = 40 h (stationary flow)

Figure 7 shows that in the homogeneous dike (Ex. 1A) the water flows in the whole region of the foot. It shows as well, that if the foot filter material is less permeable than the dike body (Ex. 1B), the water emerges above it and area 2 remains more or less dry (blue color). If, on the other hand, a higher permeability is set for the filter material, as it should be aimed for (Ex. 1C), water from the dike body gets into the filter, flows at his base and leaves the dike at edge 3 of area 2.

Table 1. Water inflow (q > 0) and outflow (q < 0) rates q [10^{-4} m²/s]

Ex.	relative permeability	Inflow waterside	Qutflow landside	
	k_{filter}/k_{dike}	Edge E7	Edge E3 foot filter	Edge E4 dike body
1A	1	1,199	-0,421	-0,763
1B	1/100	1,140	0,000	-1,111
1C	100	1,499	-1,756	0,000

In Table 1 water inflow rates (q > 0) and outflow rates (q < 0) [10^{-4} m²/s] at the boundaries during the stationary state are documented. The inflow on the water side (edge E7) of the dike is compared to the outflow on the land side. The latter consists of two parts, the outflow from the dike body (edge E4) and that from the foot filter (edge E3).

Table 1 shows that $\Sigma q \approx 0$ applies to all examples, that indicates stationary flow. Furthermore, the inflow rate as well as the sum of the outflow rate increase with the permeability of the material in area 2. The effect of the relative permeability of the foot filter material (area 2) can be seen in a different distribution of the outflow rates in Table 1. In the homogeneous dike (Ex. 1A), outflow occurs from both land side areas (edges E3 & E4). If the permeability of area 2 is lower (Ex. 1B), the water escapes solely above the foot filter (edge E4) and in edge E3 q reads zero. If the permeability of area 2 is higher (Ex. 1C), the water escapes solely from the foot filter (edge E3) and in edge E4 q reads zero.

It should be mentioned that according to the Dirichlet boundary condition, also in E6 and E7 inflow and outflow rates of water have been calculated, but as it could be expected they are very low compared to the one presented in Table 1. According to the natural boundary condition in E1 and E2 their flow rates are definitely zero.

4 MODELING OF SUFFUSION

In a first step, we consider a rigid grain skeleton, which could only be valid if the percentage of fine particles is limited. Suffusion means that fine particles of the soil (P), are solved from the grain skeleton and transported away as a result of groundwater flow. This is an erosive process in which two phases in a grain skeleton move at their own velocity. Even if the particles cannot be described as liquid without further ado, the process may still be treated as a two-phase flow with two fluid phases, so that some of the approaches from water and air flow in the grain skeleton could be used. In both cases, groundwater flow is included as a special case. However, the two models also have essential differences, which are summarized in Table 2.

The differences originate from the different physical properties of the phases (gas respective particles) and their mechanical interactions with the water and grain skeleton. So, unlike air, particles are incompressible and have no surface tension to water. Therefore, the pressure in the particle phase does not depend on its density and does not contain capillary forces and therefor no suction-saturation equation.

Unlike flow of air and water in soil, there is a mass exchange between the particles and the grain skeleton during suffusion (Askamp, 2024). This leads to an extension of the constitutive equation in order to modify the permeabilities (Buscher & Perau, 2021).

The resistance terms in the interaction term (Eq. 8) are intended to represent the filtering process and the resistance to the penetration of a suspension in the grain skeleton (BAW, 2015). In the interaction of water and particles, also surface friction is taken into account (Buscher, 2022).

Different from Potthoff (2003) the interaction forces between water and particles no longer could be neglected.

Table 2. Comparison of the constitutive relationships of the two two-phase flow models (Kagermeier u.a. 2025)

Terms for the model „water and air"	**Terms for the model „water and particles"**
$m_G = 0$ Means no mass exchange between water and air.	$m_P = f(n_F, n_P, \mathbf{w_F})$ Describes the removal of particles from the grain skeleton and their deposition (Askamp 2024).
$\mathbf{T}_F = -n_F p_{FR}\mathrm{I} + n_F F_{CF}(n_F, n_G)\mathrm{I}$ Sum of the negative hydrostatic partial pressure and a capillarity function (F_{CF}) as a function of the volume fractions of the fluids; due to the incompressibility of water, $\mathbf{T_F}$ is formulated as hydrostatic pressure and not as a function of density	$\mathbf{T_F} = -n_F p_{FR}\mathrm{I}$ Negative hydrostatic partial pressure; suction stresses do not occur due to the lack of surface tension between the phases
$\mathbf{T_G} = -n_G p_{GR}\mathrm{I} = -n_G RT\rho_{GR}\mathrm{I}$ Stress tensor consists of a hydrostatic pressure, which depends linearly on density of the air (Boyle-Mariotte's law with RT as proportionality constant)	$\mathbf{T_P} = -n_P p_{FR}\mathrm{I} - n_P \cdot \mathbf{D}_{Disp}(n_F, \mathbf{w}_F)$ Stress tensor consists of the real pressure corresponding to the pressure of the surrounding water and a component ($\mathbf{D}_{Disp}$) that takes the dispersion of the particles into account
$R_{FS} = f(n_F, n_G, K, \eta_F)$ Takes into account the interaction between water and grain skeleton; takes into account Darcy's law; leads to the calculation of the flow force; reduction of permeability in the case of partial saturation	$R_{FS} = f(n_F, n_P, K, \eta_F)$ Takes into account the interaction between water and grain skeleton; it contains Darcy's law and the Kozeny-Carman equation; leads to the calculation of the seepage forces
$R_{SG} = f(n_F, n_G, K, \eta_G)$ Takes into account the interaction between grain skeleton and air; takes into account Darcy's law; reduction of permeability at partial saturation	$R_{SP} = f(n_F, n_P, \eta_F, K)$ Describes the resistance of the grain skeleton to the movement of the particles (see Buscher & Perau 2025): • for small d_P: behavior similar to a suspension (K,$\eta_{Susp.}$) • for large d_P: geometric filter criterion
$R_{FG} = 0$ (see Potthoff, 2003) Takes into account the interaction between water and air due to relative movement, see Perau (2001)	$R_{FP} = f(n_F, n_P, \eta_F, d_P)$ Describes the resistance between particles and water (e.g. frictional force according to Stokes) (Buscher 2022), for very small particles d_P: it occurs no separation of F and P

where: η_k = Viscosity of the constituent k; K = intrinsic permeability, d_P = particle diameter, D_S = pore channel diameter

5 DISPERSION

The consideration of dispersion is essential for a realistic representation of particle transport in soil. Without the dispersive component, the spreading of particles would be limited to pure advection, which would result in unrealistically sharp concentration distributions.

As shown in Figure 2 after Ziems (1968) and Busch et al. (1983), transition zones occur at material interfaces — particularly in the case of horizontal or vertical layering of soils with different grain sizes — where fine particles penetrate into adjacent, coarse-grained zones. Such processes can only be captured by accounting for transverse dispersion.

Even in simulations involving a homogeneous soil structure, it becomes evident that without dispersion, a realistic distribution or mixing of phases at interfaces or within heterogeneous structures cannot be represented.

5.1 *Exemplary Visualization of Particle Dispersion*

Figure 8 illustrates the temporal spreading of fine particles in a homogeneous steady-state groundwater flow field with horizontal flow direction (see blue arrow), based on the work of Perau & Abdulrahman (2025).

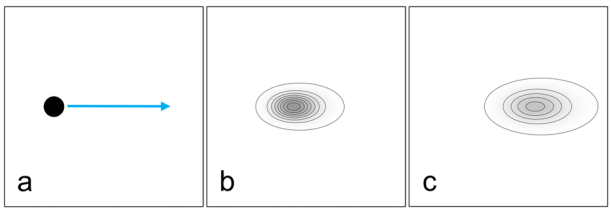

Figure 8. a) Initial concentration; b) onset of longitudinal and transverse dispersion; c) pronounced anisotropic spreading

Starting from a concentrated initial distribution, the particles spread through advection in the direction of flow. At the same time, longitudinal dispersion causes elongation along the flow direction, whereas transverse dispersion widens the concentration perpendicular to the flow direction. The interaction of both dispersion directions results in an anisotropic ellipsoidal spreading of the concentration over time.

Dispersion refers to the spatial spreading of fine particles due to fluid flow in a porous medium. Due to the pore structure, particles do not follow streamlines exactly but are deflected along their path through the grain skeleton. As a result, their concentration spreads across the flow domain over time. Dispersion is strongly influenced by the filtration velocity, pore structure and the direction and uniformity of flow.

5.2 *Example: Horizontally Layered Soil Structure*

Figure 9 shows a horizontally layered soil structure consisting of a coarse-grained material (e.g., gravel) in the upper layer and a fine-grained material (e.g., fine sand) in the lower layer. The layering runs parallel to the groundwater flow from left to right. The potential profile remains constant over time, which results in a homogeneous steady state flow field.

This example corresponds to ‘type 3/2’ after Ziems (1968) (see Figure 2), in which the flow runs horizontally and parallel to the interface between two materials with differing grain sizes. Due to the varying pore sizes, the hydraulic conductivity differs significantly: The permeability coefficient k and in consequence the filtration velocity v are much higher in the coarse material than in the fine.

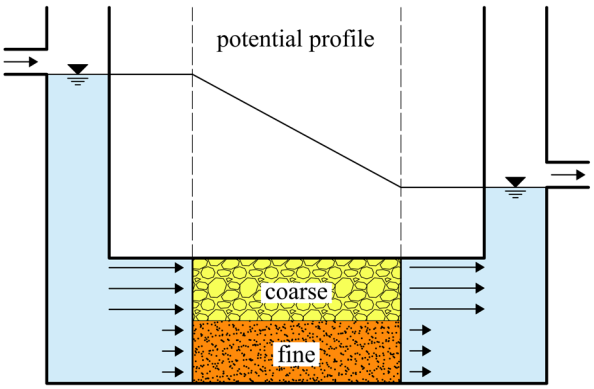

Figure 9. Horizontal flow under constant gradient in layered soil with coarse over fine material (‘type 3/2’) (Ziems, 1968)

Without considering dispersion, the interface between the two materials would remain sharp, as no particle movement from the fine to the coarse material could occur. In reality, however, transverse dispersion causes fine particles near the contact zone to migrate perpendicular to the flow direction, i.e., upwards into the coarse-grained material.

5.3 *Comparison with Dissolved Contaminants*

A similar mechanism like the particle transport mentioned above is described in the literature for dissolved contaminant transport in soils (Bear & Verruijt, 1998). However, these studies typically consider substances dissolved in water, whose transport is governed by advection, molecular diffusion and hydrodynamic dispersion.

Figure 8 shows the result of a rather simple initial boundary value problem on this contaminant transport. It is generated by a python program code, which had been developed AI-supported. For more details of this development and examples see Perau & Abdulrahman (2025).

5.4 *Mathematical Description*

In the mathematical formulation, the transport mechanism of advection and dispersion of particles can be modeled by an expression of the particles’ stress tensor $\mathbf{T_P}$, which divergence decomposes into an advective and a dispersive component:

$$div\mathbf{T}_P = div\left(-n_P \cdot p_{FR} \cdot \mathbf{I} - n_P \cdot \mathbf{D}_{\text{Disp}}\right) \tag{9}$$

where: advective component: $-n_P \cdot p_{FR} \cdot \mathbf{I}$

dispersive component: $-n_P \cdot \mathbf{D}_{\text{Disp}}$

The dispersion matrix $\mathbf{D}_{\text{Disp}}$ accounts for both, longitudinal and transverse dispersion and depends on the mass flow density of water $\mathbf{w}_F$:

$$\mathbf{D}_{\text{Disp}} = \frac{\alpha_T}{n_F \cdot \rho_{FR}} \cdot \left|\mathbf{w}_F\right| \cdot \mathbf{I} + \frac{\alpha_L - \alpha_T}{n_F \cdot \rho_{FR}} \cdot \frac{1}{\left|\mathbf{w}_F\right|} \cdot \left(\mathbf{w}_F \cdot \mathbf{w}_F^{\,\mathrm{T}}\right) \tag{10}$$

where $\mathbf{w}_F \cdot \mathbf{w}_F^{\,\mathrm{T}}$ is a dyadic product and the coefficients α_L and α_T denote the longitudinal and transverse dispersion coefficients respectively.

Beyond very small contaminants even fine soil particles are subjected to additional effects such as filtration and grain-fluid interactions, which make their transport behavior more complex. These effects have to be taken into account by the terms for R_{SP} and R_{FP}, presented in Table 2.

6 CONCLUSIONS

It has been demonstrated that existing approaches to consider suffusion only represent design rules or describe states, rather than processes. Furthermore, these approaches are limited in terms of geometry and flow direction.

As an alternative, the description of internal erosion as a process was approached using a formulation with mechanically motivated equations. The movement of groundwater and particles was interpreted as two-phase flow, so it could be treated in the same way as the flow of water and air in the soil. Therefore, existing approaches can be used to set up and solve the differential equations and constitutive relationships numerically.

The Mixed Finite Element Method was used to solve the equations for the two-phase flow of water and air, taking the mass flow densities into account as process variables. Furthermore, a preprocessor was formulated for the definition of initial boundary value problems, which is then used by the Finite Element Method (FEM) program.

The constellation of mechanical equations, FEM program and preprocessor were examined for functionality and plausibility using a varied example of two-phase flow with water and air, an inhomogeneous dike. This calculation produced results that were consistently credible. Therefore, it appears possible to transfer the entire constellation to the two-phase flow of water and particles in order to model the process of internal erosion**.**

The two-phase flows water/air and water/particles have both similarities but also significant differences. While the structure of the equations is identical, the physical properties of the phases and the interactions of these phases in particular require a different formulation. One difference in the formulation of the stress state in modeling particle flow is to include dispersion as a phenomenon. This realization has already been the result of a mental experiment.

The approach used to capture dispersion can be derived from the description of the same effect in the dispersion of dissolved contaminants in the subsurface. However, to describe the dispersion of particles in soil, it must also be taken into account that their size prevents them from easily passing through the smaller pores of the grain structure. Macroscopically, this means that the grain skeleton resists the particle movement.

In order to proceed with the modeling of the water-particle flow, it is necessary to establish the constitutive relationships in greater detail. It is also necessary to formulate suitable boundary conditions for the underlying boundary value problems. Furthermore, it is imperative to identify the parameters and formulate a series of tests. As part of the numerical implementation, the corresponding system matrices must be derived and assembled.

Finally, the approaches developed for the two-phase flow of water/particles are to be tested using suitable examples and further developed if necessary.

7 REFERENCES

Askamp, T. (2024): *Ein Modell zur Beschreibung innerer Erosion – Grundzüge des mechanischen Modells und Ansätze zum Massenproduktionsterm*. (Diss.), Universität Duisburg-Essen, Report Geotechnik, Heft 49, DOI: 10.17185/duepublico/81891

Bear, J., Verruijt, A. (1998): *Modeling Groundwater Flow and Pollution, Theory and Applications of Transport in Porous Media*, 2nd Edition, Dordrecht a.o., D. Reidel Publishing Company

Bundesanstalt für Wasserbau (Ed.) (2013a): *BAWMerkblatt Materialtransport im Boden (MMB*), Bundesanstalt für Wasserbau, Karlsruhe

Bundesanstalt für Wasserbau (Ed.) (2013b): *BAWMerkblatt Standsicherheit von Dämmen an Bundeswasserstraßen (MSD)*, Bundesanstalt für Wasserbau, Karlsruhe

Busch, K., Luckner, L., Tiemer, K. (1993): *Geohydraulik, 3*. Auflage, Berlin a.o.: Gebrüder Borntraeger

Buscher, S., Perau, E. (2021): Modellierung von Erosion und Transport von Bodenpartikeln im Korngefüge: Motivation und Konzept. In: Deutsche Gesellschaft für Geotechnik (Ed.): Fachsektionstage Geotechnik. 3. Bodenmechanik-Tagung vom 21.04.2021. Würzburg

Ehlers, W. (1989): *Poröse Medien, ein kontinuumsmechanisches Modell auf der Basis der Mischungstheorie*. Forschungsberichte aus dem Fachbereich Bauwesen, Universität Gesamthochschule Essen, Heft 47, Essen

Kagermeier, L., Buscher, S., Perau, E., Hülsbusch, J. (2025): Modellierung innerer Suffosion in Analogie zur Zweiphasenströmung von Luft und Wasser, Fachsektionstage Geotechnik, September 2025 in Würzburg, 6 pages, (to appear)

Korsawe, J., Perau, E., Potthoff, S., Starke, G. (2003): *Numerical Approximation of Water-Air Two-Phase Flow by Mixed Finite Methods*. Computers and Geotechnics 30, pp. 695-705 https://doi.org/10.1016/j.compgeo.2003.07.001

Perau, E. (2001): Die Phasen des Bodens und ihre mechanischen Wechselwirkungen. Ein Konzept zur Mechanik teilgesättigter Böden. Habilitation. Universität Essen, Essen. Fachgebiet Grundbau und Bodenmechanik, version 2020: DOI: 10.17185/duepublico/73533

Perau, E., Kagermeier, L. (2024): *Strömung von Luft und Wasser im Boden – Lösung einfacher Anfangs-Randwertprobleme mit der Gemischten FEM*, Kolloquium Numerik in der Geotechnik, 07.-08.11.2024, Karlsruhe, Bundesanstalt für Wasserbau (BAW), pp. 36-41; https://hdl.handle.net/20.500.11970/114167

Perau, E., Abdulrahman, A. (2025): *Szenario zur Anwendung von KI zur Visualisierung von Ansätzen zur Dispersion – Erfahrungen und Fragen*, Tagungsband zum 14. RuhrGeo-Tag – Digitalisierung in der Geotechnik, 27.03.2025 an der Universität Duisburg-Essen, Report Geotechnik, Heft 50, pp 79-96, DOI: 10.17185/duepublico/82728

Potthoff, S. (2003): *Simulation von Zweiphasen-Strömungen im Boden. Ein Programmsystem auf Basis der Gemischten Finite-Elemente-Methode*. Dissertation. Universität Duisburg-Essen, Essen. Mitteilungen aus dem Fachgebiet Grundbau und Bodenmechanik, Heft 31, version 2025: DOI: 10.17185/duepublico/83873

Raats, P. A. C. (1969): *Applications of the theory of mixtures in soil physics*. Rational Thermodynamics. Ed: Truesdell. S. 326-343. New York

Raviart, P. A., Thomas, J. (1977): *A Mixed Finite Element Method for 2-nd Order Elliptic Problems*. In: Dold, A.; Eckmann (Hrsg.): Mathematical Aspects for Finite Element Methods. Berlin: Springer Verlag, S. 292–315

Starke, G. (2000): *Least-Squares Mixed Finite Element Solution of Variably Saturated Flow Problems*. In: SIAM Journal of Scientific Computing 21. Nr. 5, pp. 1869–1885, DOI: 10.1137/S1064827 5983 39384

Sharp M., Wallis M., Deniaud F., Hersch-Burdick R., Tourment R., et al. (2013): *The International Levee Handbook*. CIRIA, pp.1349

Wan, C. F., Fell, R. (2008): *Assessing the Potential of Internal Instability and Suffusion in Embankment Dams and Their Foundations*. Journal of Geotechnical and Geoenvironmental Engineering 134 (3), S. 401–407

Ziems, J. (1968): *Beitrag zur Kontakterosion nichtbindiger Erdstoffe*. Disssertation. Technische Universität Dresden